

Transport properties of the Mo_3Sb_7 compound

C. Candolfi,* B. Lenoir, and A. Dauscher

Laboratoire de Physique des Matériaux, CNRS, Ecole Nationale Supérieure des Mines de Nancy, Nancy Université, Parc de Saurupt, 54042 Nancy Cedex, France

E. Guilmeau

CRISMAT-ENSICAEN, CNRS/UMR 6508, 6 Bd Maréchal Juin, 14050 Caen Cedex, France

J. Hejtmanek

Institute of Physics, Academy of Sciences of the Czech Republic, Cukrovarnicka 10, CZ-162 53 Praha 6, Czech Republic

J. Tobola, B. Wiendlocha, and S. Kaprzyk

Faculty of Physics and Applied Computer Science, AGH University of Science and Technology, 30-059 Krakow, Poland

(Received 11 July 2008; revised manuscript received 6 November 2008; published 16 January 2009)

The galvanomagnetic and thermoelectric properties including Hall effect, electrical resistivity, thermopower, and thermal conductivity have been studied for polycrystalline Mo_3Sb_7 . The temperature dependences of the various physical properties, measured from 2 up to 800 K, was explained supposing an important role of magnetic fluctuations significantly suppressed by the opening of a gap in the spin excitation spectrum. In addition, we propose that magnetic excitations are likely responsible for the exotic temperature dependence of the thermal conductivity in the whole temperature range. The high value of the dimensionless figure of merit ZT achieved at high temperature classifies this p -type metal as one of the best thermoelectric metal discovered up to now.

DOI: [10.1103/PhysRevB.79.035114](https://doi.org/10.1103/PhysRevB.79.035114)

PACS number(s): 72.15.Jf

I. INTRODUCTION

In the last two decades, strong experimental and theoretical efforts have been devoted to the search for prime materials for applications in power generation and device cooling.¹⁻⁵ Among them the thermoelectric converters play an important role. The efficiency at a temperature T of such thermoelectric device can be improved by increasing the thermoelectric dimensionless figure of merit at a temperature T , $ZT = S^2 T / \rho \lambda$, where S is the Seebeck coefficient or thermopower, ρ the electrical resistivity, and λ the total thermal conductivity.⁶ The conflicting requirements on thermal and electric transport properties involved by this simple formula make designing a thermoelectric material a complex task.

To tackle this problem, original theoretical guidelines were suggested in the early 1990s to drive the research into new directions with the so-called phonon glass-electron crystal (PGEC) concept.⁷ This approach led to exciting discoveries typified by the skutterudite and clathrate compounds.⁸⁻¹² Both families displayed interesting thermoelectric properties, making these compounds outstanding candidates for high-temperature thermoelectric generation.

Apart from these open crystalline structures, semiconducting materials with complex crystalline structure can represent another fruitful possibility to achieve high ZT values. In an effort to identify such materials, intermetallic Zintl phases have been proposed as a prospective class of compounds. Even though few Zintl phases have been studied up to now from a thermoelectric point of view, high ZT values have been reported in $\text{Yb}_{14}\text{MnSb}_{11}$ and $\text{Yb}_{14}\text{Mn}_{1-x}\text{Zn}_x\text{Sb}_{11}$.^{13,14} While their complex crystalline structure results in very low lattice thermal conductivity, the flexibility of the structure to accept a high number of substi-

tutions offers opportunities to precisely tune the electronic properties.

Compounds based on Mo_3Sb_7 have been considered as other promising Zintl phase for high-temperature thermoelectric applications. If Mo_3Sb_7 is a “holelike” metal, the proximity of the Fermi level to the valence bands edge suggests that an evolution to a semiconducting state can be realized by adding electrons to the structure.¹⁵⁻¹⁷ The first experimental attempt to drive the system into a semiconducting state has been made by considering the substitution of Sb by Te.¹⁵ Further investigations on these substituted materials resulted in high ZT value of ~ 0.8 at 1050 K, making this material an outstanding candidate for power generation.¹⁸ Surprisingly, the thermoelectric properties of the parent compound Mo_3Sb_7 have never been reported neither at low nor at high temperature. Since Mo_3Sb_7 can be considered as a reference material, it is of prime importance to investigate its thermal and electrical properties.

Moreover, it was recently reported that, besides BCS-like superconducting properties,¹⁹⁻²¹ this compound displays exotic low-temperature dependences of the electrical resistivity and magnetic susceptibility.^{22,23} If spin-fluctuation theory has been first called for to account for these unusual effects,²² the decisive role of complex magnetic interactions based on antiferromagnetically coupled molybdenum dimers resulting in a spin gap opening below $T^* = 50$ K is coherent with recent studies based on ^{121/123}Sb nuclear quadrupole resonance and muon spin relaxation.²⁴ Independently on the detailed description of the character and temperature evolution of the magnetic structure, both models involve the underlying role of magnetic interactions and raise the question of their influence on the physical properties of this material. In the present paper, the transport properties (including electrical

resistivity, thermopower, thermal conductivity, and Hall effect) have been explored on a polycrystalline sample of Mo_3Sb_7 in the 2–800 K temperature range.

II. EXPERIMENTAL DETAIL

Polycrystalline Mo_3Sb_7 has been prepared from high-purity starting materials (99.999% purity for both Mo powder and Sb shots) by a metallurgical route. Stoichiometric amounts of the elements were loaded into a quartz ampoule in an argon-atmosphere glove box. The ampoule was heated up to 750 °C and left at this temperature for 10 d. To ensure good homogeneity, the solid was then ground in an agate mortar into fine powders ($<100 \mu\text{m}$) that were cold pressed. The pellets were annealed at 750 °C for 7 d, then powdered again and finally densified by hot pressing using graphite dies in an argon atmosphere at 600 °C for 2 h under 51 MPa. The crystallographic structure was checked by x-ray diffraction and neutron diffraction.²³ To obtain an accurate lattice parameter by x-ray diffraction, high-purity silicon was added as an internal standard.

For the transport property studies, parallelepiped-shaped samples were cut using a diamond saw from the hot-pressed material with typical dimensions $2 \times 2 \times 10 \text{ mm}^3$. Galvanomagnetic measurements were performed from 2 up to 350 K with an ac physical properties measurement system option (PPMS Quantum design) in conjunction with a cryostat equipped with a 7 T superconducting magnet. Electrical resistivity, thermopower, and thermal conductivity were measured from 5 to 300 K using an automated closed-cycle refrigerator system. A steady-state technique has been used for the thermal properties. In the 300–800 K temperature range, the electrical resistivity was measured by a four probes technique based on the Van der Pauw method, while the thermopower was determined using a standard method. Thermal conductivity was determined by measuring the thermal diffusivity by a laser flash technique. A very good agreement was observed at 300 K between the low and high-temperature measurements. The deviation never exceeds 10%.

III. RESULTS AND DISCUSSION

A. Structural and chemical characterizations

The x-ray diffractogram obtained in the θ - 2θ mode from the Mo_3Sb_7 compound, shown in Fig. 1, displays all the peaks characteristic of the Ir_3Ge_7 structure (space group $Im\bar{3}m$). A minute amount of a secondary phase (less than 0.7% volume) constituted of pure antimony has been detected by x-ray diffraction (XRD). The lattice parameter obtained $a=9.568(8) \text{ \AA}$ is in very good agreement with that found in previous studies.^{26,27} Detailed information on the structural parameters of Mo_3Sb_7 obtained by neutron diffraction is described elsewhere.²⁵ The relative density of the sample, defined as the ratio of the measured density to the theoretical density, is 93%.

B. Transport properties

The electrical resistivity, ρ , measured as a function of the temperature is shown in Fig. 2(a). The binary Mo_3Sb_7 com-

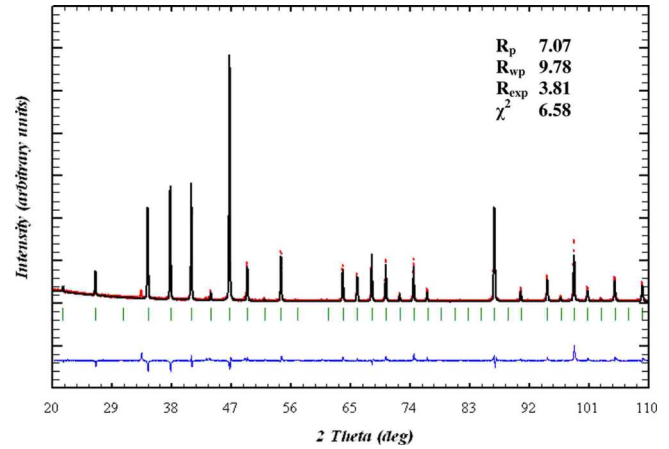


FIG. 1. (Color online) Rietveld refinement of the x-ray diffraction pattern of Mo_3Sb_7 . The only peak which is not indexed represents pure antimony.

pound exhibits a resistivity that increases as a function of temperature to reach 185 and 260 $\mu\Omega \text{ cm}$ at 300 and 800 K, respectively. This temperature dependence is metalliclike and the values encountered classify this material as a dirty metal. Moreover, we can also notice a sharp decrease of the electrical resistivity occurring at 2.25 K [Fig. 2(b)]. This de-

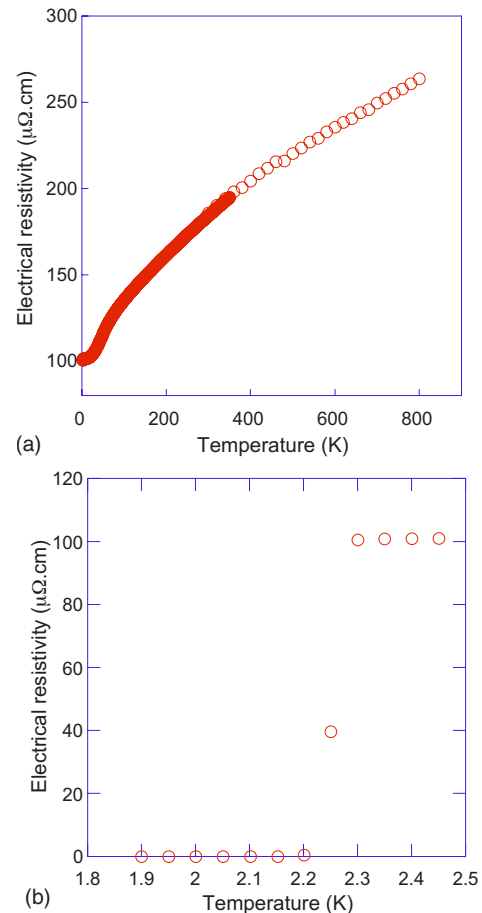


FIG. 2. (Color online) (a) Temperature dependence of the electrical resistivity. (b) Low-temperature dependence of the electrical resistivity to underline the superconducting transition.

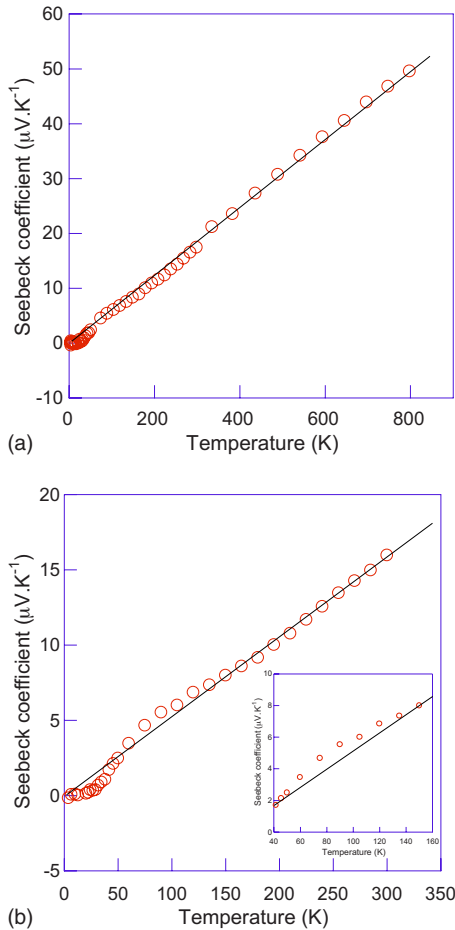


FIG. 3. (Color online) (a) Temperature dependence of the Seebeck coefficient in the 5–800 K temperature range. (b) Low-temperature evolution of the thermopower. Inset: magnification of the 40–160 K temperature range to highlight the possible phonon-drag contribution. The solid lines are a guide to the eyes to underline both the diffusive part of the thermopower and the low-temperature anomaly.

crease is unambiguously related to the superconducting transition in full agreement with previous investigations.^{21,22} If the observed low-temperature dependence has been first analyzed in view of the spin-fluctuation theory, it seems that a spin gap scenario could also be consistent with these data. However, we would like to emphasize that our measurement does not show a linear temperature dependence above 60 K as mentioned by Tran *et al.*²³ on polycrystalline sample but presents a superlinear curvature above 60 K up to 800 K.

Figures 3(a) and 3(b) display the temperature dependence of the thermopower S for the Mo_3Sb_7 compound. The Seebeck coefficient is positive indicating p -type conduction. The measured values at 300 and 800 K are 18 and 50 $\mu\text{V}/\text{K}$, respectively, the former being in quite good agreement with the value reported by Dashjav *et al.*¹⁵ The room-temperature value of Seebeck coefficient is rather high compared to metals such as Cu, Ag, or Au but is not exotic considering that high Seebeck coefficients have already been encountered in other pure elements such as in Eu, Sc, Co, Ni, or in some metallic alloys.²⁸ Let us note that due to $3d$ ($4f$) character of above mentioned elements, which exhibit unusually high

thermopower, one should insinuate the interplay between “excess” thermopower, exceeding the bare diffusive part, and magnetic excitations. This straightforward association is intensively discussed and studied, e.g., in metallic cobaltites but is far to be fully understood.^{29–31}

In addition to the classical diffusive part of the thermopower which displays impressive linear temperature dependence from 800 K down to 150 K, a broad bump reaching a maximum near 80 K appears below this temperature [see inset in Fig. 3(b)]. Such an intriguing feature is often closely related to various drag effects as phonon or magnon drag. A possible origin of this low-temperature enhancement could arise from the strong electron-phonon interaction which is present in the Mo_3Sb_7 compound.²² One could therefore suppose that a phonon-drag effect could manifest itself in the range $\sim 30\text{--}85$ K ($0.1\Theta_D\text{--}0.3\Theta_D$, where Θ_D is the Debye temperature, i.e., 285 K for the Mo_3Sb_7 compound).³² Below 50 K, another deviation from linearity occurs. The thermopower strongly decreases to reach a nearly zero value below 20 K. This behavior could be clearly related to the density of state (DOS) and its derivatives in the vicinity of E_F since a local minimum could lead to carrier compensation. However, supposing that the spin gap opens below ~ 50 K, one can naturally wonder if the anomaly revealed in the thermopower measurement is not related to this transition. Actually, the thermopower measures the entropy transported by charge carriers as it moves divided by the carrier’s charge. As the transition to a spin gap state involves a drastic change of the magnetic contribution to the specific heat, it should substantially affect the temperature dependence of the thermopower near T^* . This interesting point deserves further experimental and theoretical investigations since, to the best of our knowledge, this topic has never been addressed in the literature.

The magnetic field dependence of the Hall resistivity has also revealed unusual features. Note that to dismiss any magnetoresistance contribution, the Hall resistivities ρ_H presented here result from $[\rho_H(+B) - \rho_H(-B)]/2$, where B is the magnetic field. While at room temperature the Hall resistivity varies linearly with the magnetic field up to 7 T, we observed, below 300 K, a deviation from linearity above ~ 3 T, all the more pronounced that the temperature is low. As an example, Fig. 4(a) shows the situation for $T=5$ and 300 K. Whatever the temperature is, the linear part displays a positive slope suggesting hole conduction. It is well established that deviation from linearity can be expected in either materials displaying large localized magnetic moments or in materials where the low-field approximation ($\mu B \ll 1$, where μ is the carrier mobility and B the magnetic field) is cancelled. This last hypothesis can be rejected in Mo_3Sb_7 if one refers to its electronic band structure for which flat bands have been noticed implying a large effective mass which is not supposed to match with high carrier mobility. Retracing to the first point, since we can rule out any ferromagnetic contribution, the complex magnetic interactions of the molybdenum dimers could be then responsible for the nonlinear Hall voltage. Further experimental evidence for this hypothesis is provided by a detailed analysis of the transport data of the $\text{Mo}_3\text{Sb}_{7-x}\text{Te}_x$ compounds.³³ The variations of the transport properties together with the magnetic susceptibility as the Te

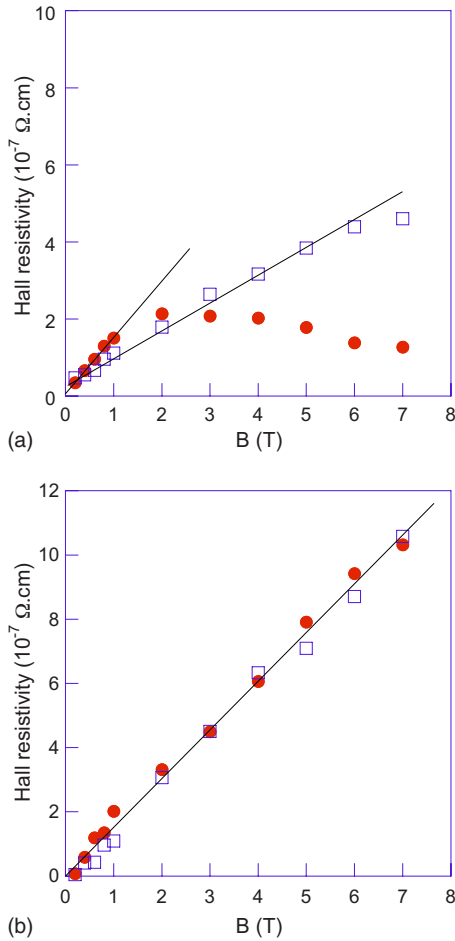


FIG. 4. (Color online) (a) Magnetic field dependence of the Hall resistivity of Mo₃Sb₇ at $T=5$ K (●) and $T=300$ K (□). The solid lines are a guide to the eyes to underline the deviation from linearity of the low-temperature data. (b) Hall resistivity as a function of the magnetic field of the Mo₃Sb_{5.4}Te_{1.6} compound at $T=5$ K (●) and $T=300$ K (□).

content increases stand for compelling evidence of a progressive suppression of the magnetic interactions. This phenomenon is concomitant with a disappearance of the nonlinear Hall voltage throughout the temperature range investigated as Fig. 4(b) attests to. Nevertheless, even though the presence of complex magnetic interactions precludes any separation of the anomalous contribution from the measured data, several characteristics can be extracted from the room-temperature data where the deviation from linearity can be neglected. Assuming that at room temperature, the simple relation relating the Hall coefficient R_H to the carrier concentration p is valid, $R_H=1/pe$, we can then estimate p and the Hall mobility $\mu_H=R_H/\rho$. From our data at 300 K, we obtained $p\sim 8.5\times 10^{21}$ cm⁻³ and $\mu_H\sim 4$ cm² V⁻¹ s⁻¹, values consistent with the “poor-metallic” character of the Mo₃Sb₇ compound.

The total measured thermal conductivity, denoted as λ_T , is plotted as a function of the temperature on Fig. 5(a). In non-magnetic materials, the thermal conductivity is generally composed of two main contributions: an electronic λ_e and a lattice contribution λ_L ,

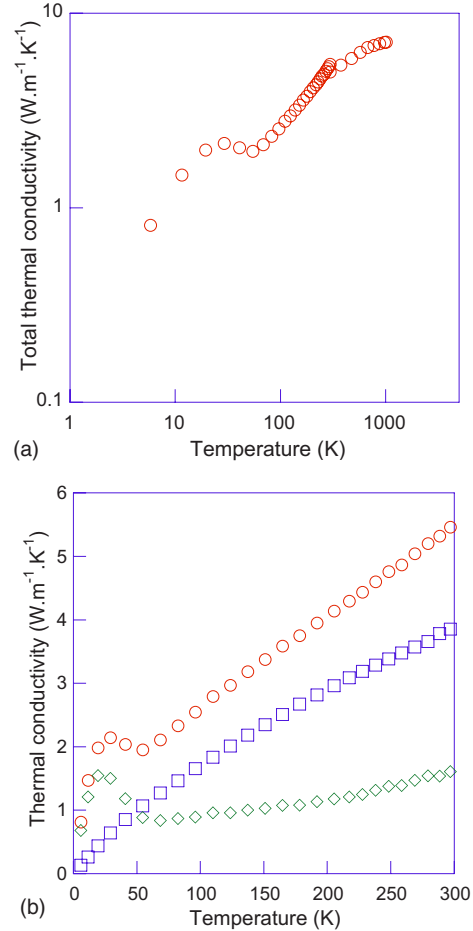


FIG. 5. (Color online) (a) Total thermal conductivity of the Mo₃Sb₇ compound in the 5–1000 K temperature range. (b) Temperature dependence of the total (○), lattice (◇), and electronic (□) thermal conductivities.

$$\lambda_T = \lambda_e + \lambda_L. \tag{1}$$

The measured thermal conductivity of the Mo₃Sb₇ compound decreases with decreasing temperature down to 50 K and below exhibits a slight maximum at 25 K to decrease sharply at lower temperature. To go further, we have estimated the lattice part of the total thermal conductivity in the 5–300 K temperature range by subtracting the electronic thermal conductivity according to the Wiedemann-Franz law

$$\lambda_e = \frac{LT}{\rho}, \tag{2}$$

where T is the absolute temperature and fixing, as a rough approximation, the Lorenz number L to the value of an electron degenerated gas, e.g., $L=L_0=2.44\times 10^{-8}$ V²/K². From this simple approach, it can be seen in Fig. 5(b) that the lattice thermal conductivity of the Mo₃Sb₇ compound is the dominant contribution below 50 K while at 300 K, it only amounts to 30% of the total thermal conductivity. It should be noted that strong deviations of L from L_0 would not essentially change neither this tendency nor the exotic temperature dependence of the lattice thermal conductivity.

To account for the unusual low-temperature dependence of the lattice thermal conductivity, it could be fruitful to consider a possible intimate interplay between magnetic interactions, the spin gap opening, and phonons. Actually, the observed behavior is qualitatively reminiscent to that reported in the spin-Peierls NaV_2O_5 compound.³⁴ In this system, a slow decrease of the total thermal conductivity by approaching the transition temperature T^* and a sharp maximum below T^* constitute the two prominent characteristics. This latter property could arise from the spin gap opening which switches off spin-phonon scattering and thus implies a more pronounced contribution of phonons to the thermal conductivity. As revealed by the Fig. 5(b), similar tendencies can be observed in the Mo_3Sb_7 compound. In addition, the mutual positions of T^* and of the temperature where the lattice thermal conductivity starts to increase seem to reinforce this picture. However, differences between these two compounds exist. The maximum value reached below T^* is significantly less pronounced in the case of Mo_3Sb_7 . This fact could be related either to the electron-phonon interaction, the complex crystalline structure, or, eventually, not completely suppressed spin scattering below T^* . Furthermore, the slow increase above T^* occurs in the 50–300 K temperature range while the same behavior becomes obvious only below 60 K in the NaV_2O_5 compound.³⁴ We can tentatively attribute this exotic dependence to a strong diffusion of phonons by the magnetic interactions of the molybdenum dimers. Further experimental evidences for this viewpoint are delivered by the thermal properties of the $\text{Mo}_3\text{Sb}_{7-x}\text{Te}_x$ compounds which will be discussed in detail elsewhere.³³

At high temperature (300–800 K), we can notice a clear saturation tendency as the temperature increases up to 1000 K. Besides this unforeseen dependence, the measured values underline the irrelevance of our hypothesis to consider $L = L_0$ since in this case λ_e at 800 K ($\sim 7 \text{ Wm}^{-1} \text{ K}^{-1}$) would account for the total measured thermal conductivity or even higher. Actually, the Lorenz number can depend on the diffusion scattering mechanisms as well as on temperature, making a separation of the two aforementioned components a complex task. Nevertheless, since the electrical resistivity increases in the whole temperature range, we can assume a similar evolution for λ_e . These facts would then result in a decrease of the lattice thermal conductivity at high temperature due to Umklapp processes. Below room temperature, the scattering would be then dominated by the dimer's magnetic interactions while they would be supplanted by phonon-phonon interactions at high temperature.

Based on the measured transport properties, the dimensionless figure of merit, ZT , can be calculated. The results are presented in Fig. 6 in the 5–800 K temperature range. The ZT values increase monotonously with increasing temperature, reaching a value of ~ 0.01 and ~ 0.11 at 300 and 800 K, respectively. These ZT values are at least 1 order of magnitude higher than in normal metals and highlight the benefic

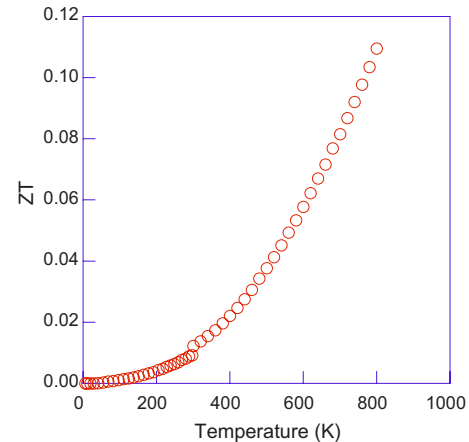


FIG. 6. (Color online) Temperature dependence of the dimensionless figure of merit ZT .

influence of tellurium on the thermoelectric properties of the Mo_3Sb_7 compound reported by Gascoin *et al.*¹⁸ To determine if further optimization of its thermoelectric properties is possible, it would be of interest to investigate other substitutions by elements richer in electrons than Mo or Sb.

IV. SUMMARY

Transport properties of the Mo_3Sb_7 compound have been measured and analyzed from 2 up to 800 K. Some anomalies in both electrical and thermal properties have been evidenced near 50 K. The exotic temperature dependence of the thermal conductivity has been tentatively interpreted by considering the presence of a spin gap below 50 K and complex Mo-Mo magnetic interactions above this temperature. This latter property could then be the dominant source of phonon diffusion below room temperature. Simultaneously, the anomalies in the thermopower temperature dependence observed below ~ 75 K could be explained supposing a close interplay between spin excitations and charge-carrier subsystem. Even though the metallic properties of Mo_3Sb_7 did not result in large thermoelectric figure of merit ZT compared to those obtained in state-of-the-art thermoelectric materials, the highest value obtained in the temperature range investigated stands for one of the best value discovered in a metal up to now. Moreover, this study can serve as a useful reference for further investigations on substituted compounds.

ACKNOWLEDGMENTS

C.C. greatly thanks M. Amiet and P. Maigné, financial support of DGA (Délégation Générale pour l'Armement, Ministry of Defense, France), and the Network of Excellence CMA (Complex Metallic Alloys). J.T. and S.K. acknowledge the support of the Polish Ministry of Science and Higher Education (Grant No. N202-2104-33). We greatly thank the experimental support of C. Bellouard.

*Corresponding author; christophe.candolfi@mines.inpl-nancy.fr

- ¹T. M. Tritt, *Science* **283**, 804 (1999).
- ²F. J. DiSalvo, *Science* **285**, 703 (1999).
- ³A. Dauscher, B. Lenoir, H. Scherrer, and T. Caillat, *Recent Research Development in Materials Science* (Research Signpost, Kerala, 2002), Vol. 3, p. 180.
- ⁴D. M. Rowe, *Thermoelectrics Handbook: Macro to Nano* (CRC Taylor & Francis, London, 2006).
- ⁵G. J. Snyder and E. S. Toberer, *Nat. Mater.* **7**, 105 (2008).
- ⁶A. F. Ioffe, *Physics of Semiconductors* (Academic, New York, 1960).
- ⁷G. A. Slack, *CRC Handbook of Thermoelectrics* (CRC, Boca Raton, FL, 1995).
- ⁸C. Uher, in *Semiconductors and Semimetals*, edited by T. M. Tritt (Academic, New York, 2000), Vol. 69, p. 139, and references therein.
- ⁹M. Puyet, A. Dauscher, B. Lenoir, C. Bellouard, C. Stiewe, E. Müller, J. Hejtmanek, and J. Tobola, *Phys. Rev. B* **75**, 245110 (2007).
- ¹⁰G. S. Nolas, J. L. Cohn, G. A. Slack, and S. B. Schujman, *Appl. Phys. Lett.* **73**, 178 (1998).
- ¹¹J. L. Cohn, G. S. Nolas, V. Fessatidis, T. H. Metcalf, and G. A. Slack, *Phys. Rev. Lett.* **82**, 779 (1999).
- ¹²G. S. Nolas, G. A. Slack, and S. B. Schujman, in *Semiconductors and Semimetals*, edited by T. M. Tritt (Academic, New York, 2001), Vol. 69, p. 255, and references therein.
- ¹³S. R. Brown, S. M. Kauzlarich, F. Gascoin, and G. J. Snyder, *Chem. Mater.* **18**, 1873 (2006).
- ¹⁴S. R. Brown, E. S. Toberer, T. Ikeda, C. A. Cox, F. Gascoin, S. M. Kauzlarich, and G. J. Snyder, *Chem. Mater.* **20**, 3412 (2008).
- ¹⁵E. Dashjav, A. Szczepińska, and H. Kleinke, *J. Mater. Chem.* **12**, 345 (2002).
- ¹⁶U. Häussermann, M. Elding-Ponten, C. Svensson, and S. Lidin, *Chem. Eur. J.* **4**, 1007 (1998).
- ¹⁷B. Wiendlocha, J. Tobola, M. Sternik, S. Kaprzyk, K. Parlinski and A. M. Oles, *Phys. Rev. B* **78**, 060507(R) (2008).
- ¹⁸F. Gascoin, J. Rasmussen, and G. J. Snyder, *J. Alloys Compd.* **427**, 324 (2007).
- ¹⁹C. Candolfi, B. Lenoir, A. Dauscher, J. Hejtmanek, E. Santava, and J. Tobola, *Phys. Rev. B* **77**, 092509 (2008).
- ²⁰R. Khasanov, P. W. Klamut, A. Shengelaya, Z. Bukowski, I. M. Savic, C. Baines, and H. Keller, *Phys. Rev. B* **78**, 014502 (2008).
- ²¹Z. Bukowski, D. Badurski, J. Stepien-Damm, and R. Troc, *Solid State Commun.* **123**, 283 (2002).
- ²²C. Candolfi, B. Lenoir, A. Dauscher, C. Bellouard, J. Hejtmanek, E. Santava, and J. Tobola, *Phys. Rev. Lett.* **99**, 037006 (2007).
- ²³V. H. Tran, W. Miiller, and Z. Bukowski, *Phys. Rev. Lett.* **100**, 137004 (2008).
- ²⁴T. Koyama, H. Yamashita, Y. Takahashi, T. Kohara, I. Watanabe, Y. Tabata, and H. Nakamura, *Phys. Rev. Lett.* **101**, 126404 (2008).
- ²⁵C. Candolfi, B. Lenoir, A. Dauscher, J. Tobola, S. J. Clarke, and R. I. Smith, *Chem. Mater.* **20**, 6556 (2008).
- ²⁶A. Brown, *Nature* (London) **206**, 502 (1965).
- ²⁷P. Jensen, A. Kjekskus, and T. Skansen, *Acta Chem. Scand.* (1947-1973) **20**, 403 (1966).
- ²⁸D. M. Rowe and C. M. Bahandri, *Modern Thermoelectrics* (Holt Saunders, London, 1983).
- ²⁹A. Wang, N. S. Rogado, R. J. Cava, and N. P. Ong, *Nature* (London) **423**, 425 (2003).
- ³⁰I. Terasaki, Y. Sasago, and K. Uchinokura, *Phys. Rev. B* **56**, R12685 (1997).
- ³¹W. Koshibae, K. Tsutsui, and S. Maekawa, *Phys. Rev. B* **62**, 6869 (2000).
- ³²This value has been obtained from sound velocity measurements and further confirmed by a detailed analysis of neutron-diffraction experiments.
- ³³C. Candolfi, B. Lenoir, A. Dauscher, E. Santava, J. Hejtmanek, and J. Tobola (unpublished).
- ³⁴A. N. Vasil'ev, V. V. Pryadun, D. I. Khomskii, G. Dhalenne, A. Revcolevschi, M. Isobe, and Y. Ueda, *Phys. Rev. Lett.* **81**, 1949 (1998).